Available online at www.sciencedirect.com
ScienceDirect
Journal of Nuclear Materials 362 (2007) 431–437
journal of nuclear materials
www.elsevier.com/locate/jnucmat

Helium release from plutonium and curium-doped zirconolite

T. Wiss [a,*], X. Deschanels [b], J.-P. Hiernaut [a], D. Roudil [b], S. Peuget [b], V.V. Rondinella [a]

[a] European Commission, Joint Research Centre, Institute for Transuranium Elements, P.O. Box 2340, 76125 Karlsruhe, Germany
[b] Commissariat à l'Energie Atomique, Centre de VALRHO, B.P. 30207 Bagnols-sur-Cèze, France

Abstract

Synthetic zirconolite compounds ($CaZrTi_2O_7$) were fabricated and doped with either the short lived alpha-emitters ^{244}Cm (half-life of 18.11 yr) or ^{238}Pu (half-life: 87.7 yr), or with ^{239}Pu (half-life of 24 110 yr) to generate various amounts of helium and of alpha-damage over laboratory time scale. The samples were annealed in a Knudsen cell, and the helium release profiles interpreted in conjunction with parallel radiation damage and previous annealing behaviour studies. The helium released during the annealing was quantitatively analysed, providing insight on the helium confinement capacity of the zirconolite material.

PACS: 51.20.+d; 61.72.Ww

1. Introduction

In the early stages of the civilian nuclear power industry the strategy for the handling of the high-level radioactive waste (HLW) was to immobilize them in borosilicate glass, followed by disposal in deep geological repositories. Alternative disposal matrices (waste forms) were considered with the basic idea of incorporating the waste fission products and associated actinides but also excess of weapons plutonium (in the United States) in the crystalline lattices of synthetic minerals, which were known to be very long-lived (many millions of years) in nature [1]. These minerals included silicates, phosphates (monazite, apatite).

In 1979, Ringwood et al. [2] suggested that mixtures of titanate minerals could be used to incorporate HLW, on the basis that titanates are water-resistant. Because of the resemblance of the titanate phases to naturally occurring rocks, the alternate material was called SYNROC (synthetic-rock). Several forms of SYNROC have been named but the most extensively studied is SYNROC-C which was designed to incorporate Purex-type reprocessing waste from commercial nuclear power production [3]. SYNROC-C consists of four main titanate phases, ziconolite ($CaZrTi_2O_7$), 'hollandite' ($Ba(Al,Ti)_2Ti_6O_{16}$), perovskite ($CaTiO_3$), titanium oxides (Ti_xO_{2x-1}) and ~2–5% metallic alloys. The first three phases provide various lattice sites in which nearly all the HLW ions are incorporated in solid

* Corresponding author. Tel.: +49 7247 951 447; fax: +49 7247 951 99447.
E-mail address: Thierry.wiss@ec.europa.eu (T. Wiss).

0022-3115/$ - see front matter © 2007 Elsevier B.V. All rights reserved.
doi:10.1016/j.jnucmat.2007.01.096

solution. Titanium oxides are important – although they do not incorporate waste elements, they provide a chemical buffer that enables the relative proportion of SYNROC phases to vary in an in-situ manner.

Zirconolite is a key phase capable of incorporating actinides (such as U, Np and Pu). It has a layered structure that exhibits a range of stoichiometries and polytypes, described by the general formula $CaZr_xTi_{3-x}O_7$. The polytype most commonly referred to as zirconolite is zirconolite-2M. This is monoclinic, has a two layer repeat and displays $CaZr_xTi_{3-x}O_7$ stoichiometry for $0.80 < x < 1.37$. The Ca site in zirconolite-2M is eight coordinated, the Zr-site is seven coordinated and there are three distinct Ti sites, two of which are six-coordinated and the third, half-occupied site, five coordinated. Rare-earth and actinide elements may be incorporated on either the Ca or Zr sites depending on the charge compensation required. The following compounds have therefore been considered in this study: zirconolite ($CaZrTi_2O_7$) of the monoclinic structure doped either with Cm or with Pu.

However, the long term behaviour of such containment matrices is strongly affected by radiogenic helium formation as well as by self-irradiation effects due to radioactive decay of the incorporated actinides. Ascertaining whether the helium generated in these materials can be accommodated in the lattice or at trapping sites without adversely affecting the material integrity or whether helium will migrate, possibly increasing the pressure on the next confinement barriers is of major importance to overall waste package behaviour. Precipitation of helium in bubbles in conjunction with phase change/amorphization might induce macroscopic swelling and cracking of the material. The resulting increase of surface to volume ratio would significantly affect the leaching behaviour of this confinement matrix.

Many studies have been previously performed on metamict minerals [4,5] on synthetic compounds doped with short lived actinides [6–8] and also to ion irradiation [4,9,10]. The kinetic effects governing the overall damage build-up are not really considered in this study since the actinides incorporated are short living ones. Indeed, in most of the cases it is also difficult to trace the geological history of natural occurring minerals and more particularly the temperature history.

Previously, little attention was paid on the possible effects of radiogenic helium on the matrix stability and mechanical behaviour and it is therefore considered in this study in conjunction with damage build-up.

2. Experimental procedure

2.1. The samples

The material doped with ^{244}Cm (half-life of 18.1 yr) was prepared from zirconyl nitrate, calcium carbonate and titanate. A more detailed description can be found in Ref. [11]. The total quantity of helium generated in the sample between its synthesis and the annealing experiment was calculated using the Nuclides.net code [12]. The change in composition must be accounted for when analyzing the specimens. At the fabrication the dopant was already constituted of a mix of ^{244}Cm containing about 17% of ^{240}Pu. This fraction has evolved to 62% for the plutonium at the time the release experiments were performed.

The samples doped with ^{238}Pu and ^{239}Pu have been obtained by mixing PuO_2 with an inactive precursor's fabricated by a sol–gel process. A more precise description of this process can be found in Ref. [13]. The substitution of aluminium for titanium compensates the excess cationic charge resulting from the incorporation of plutonium. The final composition of the samples was $Ca_{0.87}Pu_{0.13}ZrAl_{0.26}Ti_{1.74}O_7$.

The helium generated in the specimens reached a specific helium concentration of 6×10^{16}, 5×10^{18} and $4 \times 10^{19}\ g^{-1}$ for the zirconolites doped with ^{239}Pu, ^{238}Pu and ^{244}Cm, respectively.

2.2. The devices

Helium release measurements have been carried out in a Knudsen cell facility equipped with a quadrupole mass-spectrometer (KCMS). The device is installed in a shielded glove-box for the safe handling of radioactive materials. The samples are placed in a tungsten cell and are heated, under high vacuum conditions, up to 2000 K using a heating ramp of 10 or 30 K min^{-1}. The helium released from the sample effuse through the Knudsen cell orifice and is measured on line by mass spectrometry. A direct semi-quantitative evaluation of the gas is possible with the KCMS, a quantitative analysis can only be perform by adjunction of the equipment (Q-GAMES) that measures the released gas together with a spike [14]. The release profiles were evaluated as functions

of time/temperature. The normalized fractional helium release (NFR) was calculated since the samples all started to melt therefore assuming that the whole helium has been released.

Transmission electron microscopy was performed on the Cm-doped specimens using a TEM H700 HST from Hitachi. The samples were crushed in a mortar in ethanol and the resulting suspension was dropped onto a TEM copper grid coated with carbon. The TEM has been modified allowing the handling of radioactive materials.

3. Results

Fig. 1 shows the release curves for the three zirconolite samples. At first sight it is remarkable how the specimens containing high quantities of helium behave qualitatively similarly and this irrespectively from the fact that the samples have been doped with Cm or with Pu and also independently from the fabrication route. In the case of the sample doped with Cm the helium has been accumulated for ~20 yr whereas for the Pu-doped zirconolite it was only 3.5 yr. However, the profiles of the ^{244}Cm-doped and ^{238}Pu-doped samples are shifted by 100 K. This effect has been observed when the heating ramp was varied from 10 to 30 K min^{-1}.

The helium release of the two specimens containing the highest gas quantities starts at 600 K and peaks at ~800 K. A descending phase is observed during the next 100 K before a sudden release peaking at 900 and 1000 K for the material doped with ^{244}Cm and ^{238}Pu, respectively. Over the following 300 K the release profile shows a moderate slight increase until 1200 and 1300 K for the zirconolite doped with ^{244}Cm and ^{238}Pu, respectively. The release is stopped and only a little fraction is released again at 1600 and 1700 K for the sample doped with ^{244}Cm and ^{238}Pu, respectively. It is around 1700 K that the main helium release from the zirconolite doped with ^{239}Pu occurs. It can be noted that although the samples have cumulated about ten times more helium for the Cm-doped one the signal is of the same magnitude than that of the ^{238}Pu-doped sample due to the use of a quantity about ten times lower for the former.

Fig. 2 shows the normalized fractional release (NFR) from the three compounds studied. It is noticeable that the main release from the specimen doped with the short lived actinides ^{244}Cm and ^{238}Pu is mostly finished at 1000 K whereas the release suddenly starts at only 1700 K for the sample doped with ^{239}Pu.

Fig. 3 shows a TEM micrograph of an electron beam recrystallised zirconolite sample doped with

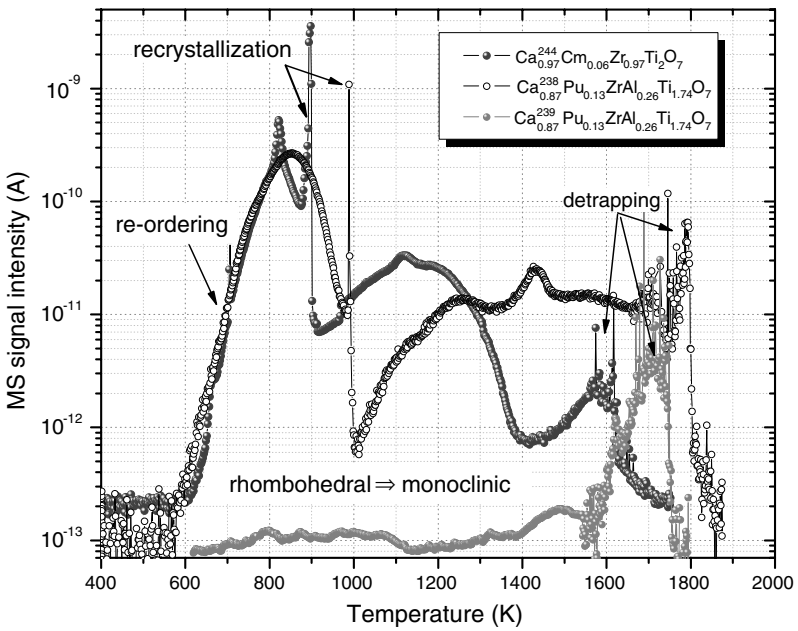

Fig. 1. Helium mass-spectrometer signal (MS) during thermal annealing of zirconolite specimens doped with ^{239}Pu, ^{238}Pu and ^{244}Cm. The cumulated α-doses for the ^{239}Pu, ^{238}Pu and ^{244}Cm-doped specimens at the time of the experiment were, respectively, 6×10^{16}, 5×10^{18} and 4×10^{19} g^{-1}.

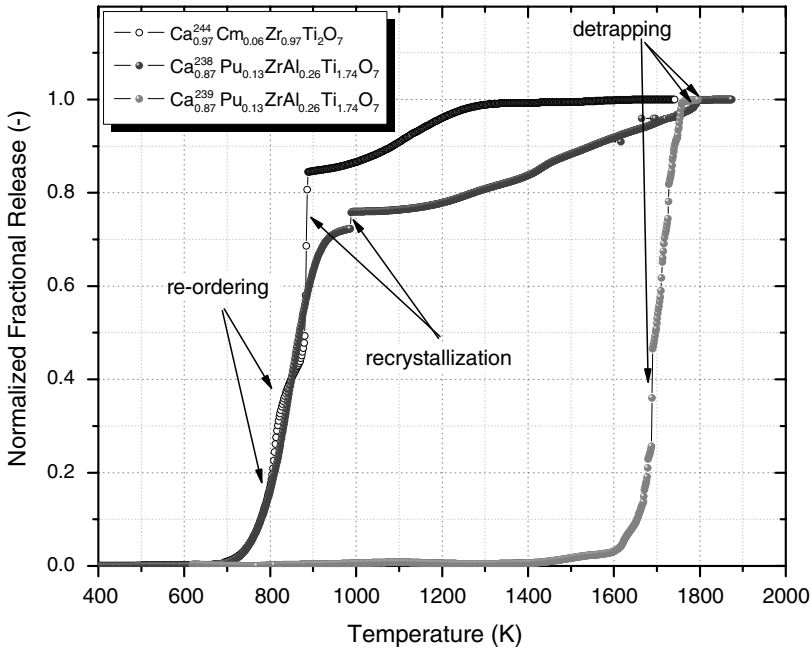

Fig. 2. Normalized fractional release (NFR) during thermal annealing of zirconolite specimens doped with ^{239}Pu, ^{238}Pu and ^{244}Cm.

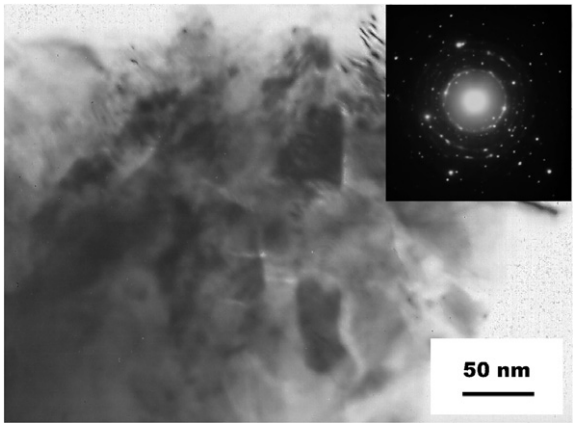

Fig. 3. TEM micrographs of the zirconolite doped with ^{244}Cm showing the electron beam recrystallised structure with grains sizing between 10 and 50 nm (original size between 10 and 100 μm). The selective area diffraction pattern in the inset confirms the presence of numerous grains in the area.

^{244}Cm after amorphisation at an α-dose of 2.3×10^{25} m^{-3}. The subsequent electron beam recrystallised material shows a microstructure with grains sizing between 10 and 50 nm (original size between 10 and 100 μm). The selective area diffraction pattern in the inset confirms the presence of numerous grains in the area. This phenomenon has been observed in many compounds when thin areas are exposed to electron beam [15] and in many metamict minerals as observed by Ewing and Headley for *e.g.* [16].

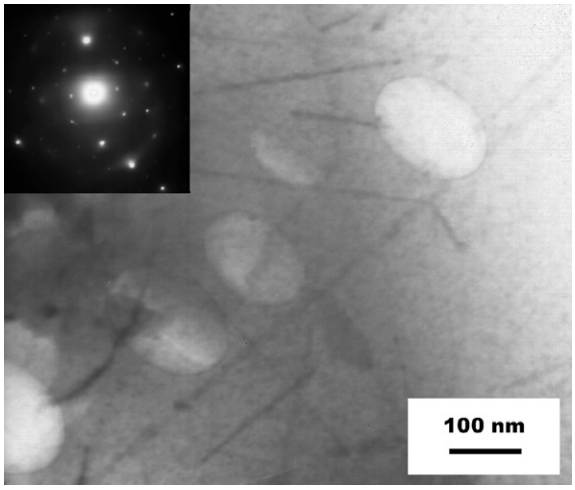

Fig. 4. TEM micrograph showing the presence of tracks from the spontaneous fission from ^{244}Cm. It has been calculated that these events are not sufficient to cause overlap of amorphous tracks as observed in TEM. The volume of the tracks is negligible in the total volume of the sample. Amorphisation is mainly due to the dense cascades of the alpha-decaying actinides. At the α-dose of 2.5×10^{18} g^{-1} the diffraction pattern confirms the presence of a diffuse radial ring is visible together with some remaining crystallites. The micrograph also shows the presence of pores of about 100 nm.

A TEM micrograph evidencing the presence of tracks from the spontaneous fission from ^{244}Cm is shown in Fig. 4. It has been calculated that these events are not sufficient to cause overlap of amorphous tracks as observed in TEM. The volume of the tracks is negligible in the total volume of the sample (2–3%). Amorphisation is attributed mainly to the dense cascades of the alpha-decaying actinides. At the α-dose of 2.5×10^{18} g^{-1} a diffuse radial ring is visible in the diffraction pattern confirming the presence of an amorphous phase together with some remaining crystallites evidenced by some diffraction spot in the SAED pattern. The micrograph also shows some pores sizing about 100 nm. The presence of such pores might be trapping sites for helium produced in the specimens.

4. Discussion

The helium release from actinide doped zirconolite specimens was shown to start at relatively low temperature for the samples having cumulated high damage dose and corresponding high quantities of radiogenic helium (samples doped with ^{238}Pu and with ^{244}Cm). The compound doped with ^{239}Pu contained ~100 times less helium than the one doped with ^{238}Pu and the release of helium was only noticeable above 1700 K, a temperature at which most of the helium from the other compounds was released. Several aspects have been considered in the analysis of the release curves.

The damage build-up from the alpha decays of the incorporated actinides was shown to amorphise the zirconolite at a critical dose. The amorphisation α-dose threshold of the Cm-doped zirconolite was determined to be around 2.2×10^{25} m^{-3} corresponding to an α-dose per mass unit of 3.9×10^{18} g^{-1} [6]. This amorphisation dose has been obtained by averaging the close amorphisation α-doses observed by XRD (2.1×10^{25} m^{-3}) and by TEM analysis (2.3×10^{25} m^{-3}). Fig. 3 shows a TEM micrograph of a Cm-doped zirconolite fragment recorded after an α-dose accumulation of $\sim 4 \times 10^{18}$ g^{-1}. This dose corresponds precisely to the required dose for complete amorphisation of the zirconolite. The TEM micrograph in this case shows an electron beam recrystallised pattern from the original amorphous sample. Very similarly, a critical α-dose for amorphisation of 4×10^{18} g^{-1} was determined by XRD for the ^{238}Pu-doped ceramic [17]. The amorphisation of zirconolite has also been determined from annealing studies by monitoring the isochronal recovery of the swelling observed in Cm-doped zirconolite [6] and from observations made on cubic (pyrochlore structure) $CaPuTi_2O_7$ and on Pu-doped $CaZrTi_2O_7$ [7,18,19] In summary it was found that the recovery of the original structure for the Cm-doped zirconolite occurs in many steps. The first one is associated with the recrystallisation from the amorphous state into a rhombohedral (pseudo-cubic) structure between 850 and 1120 K and then with the final restructuring into the monoclinic form at 1320 K. More details of the XRD annealing studies can be found in Ref. [6]. The damage recovery was also studied from the macroscopic swelling regression during annealing. The swelling associated to a full amorphous state was measured to be ~4.2% at 725 K and up to 6% for samples stored at 325 K. These values are in good agreement with those published by Clinard et al. [19] quoting ~4.3% and ~5.4% for $CaPuTi_2O_7$ stored at 340 K and 570 K, respectively. It was observed that when stored at 870 K (corresponding to the recrystallisation temperature) the zirconolite remains crystalline. In our study it can therefore be postulated that the samples doped with ^{244}Cm and with ^{238}Pu were amorphous at the time they where analyzed in the Knudsen cell. The sample doped with ^{239}Pu was indeed still crystalline and the differences in the release profile are imputable to a crystalline compound.

By integrating these numerous and coherent observations with the helium release profiles it can be assumed that the onset (at 600 K) for helium release in the ^{238}Pu and ^{244}Cm-doped zirconolite is associated with the re-ordering of the amorphous material. This first re-ordering occurs in a pseudo-cubic form which might present some structural vacancies (rhombohedral) as observed in the XRD annealing of the ^{244}Cm-doped specimens by Weber et al. [6]. The sharp release peak in Fig. 1 also evident by the sharp increase in the fractional release curve in Fig. 2 is attributed to the full recrystallisation of the material. The shift in temperature is possibly associated to a difference in recrystallisation temperature due to the difference in composition of the two materials even if qualitatively the profiles are identical. In the subsequent part of the release curve (900–1400 K and 1000–1600 K for the ^{244}Cm-doped and ^{238}Pu-doped materials, respectively) the release is attributed to the transformation from the pseudo-cubic form back to the original monoclinic structure of the zirconolite associated to a smaller unit cell volume. The last fraction

released occurs at about 1600 K for the ^{244}Cm-doped material and at 1700 K for both ^{238}Pu- and ^{239}Pu-doped samples. In the later case it is even the only noticeable release peak. The release in this case is attributed to the remaining helium dissolved/trapped in the zirconolite structure. As shown in Fig. 4, the presence of some pores in the ^{244}Cm-doped specimens might be trapping sites for the helium explaining the burst liked shape release of helium at higher temperature.

Some remarks should be made on the kinetic aspects of helium build-up and the corresponding damage build-up. The natural occurring zirconolites shows a variable behaviour. Vlasov [20] reports a density difference of ~8% for metamict zirconolites and Ewing and Headley [16] announce an α-dose of $3–10 \times 10^{25}$ m^{-3} to observe amorphisation in the TEM, close to what is observed in our actinide doped-synthetic compounds. On contrary, Sinclair and Ringwood [21] report that natural zirconolites remained crystalline after an α-dose of 3.7×10^{27} m^{-3}. It is however evident that the thermal history plays a major effect in the recovery/amorphisation process. Since the helium release starts at a temperature at which the amorphisation process is possible it can not be accurately assessed whether helium generated in a matrix stored close to this critical temperature would remain in the structure or not. Indeed the temperature in a repository could reach 500 K, which is below the onset for release but nevertheless not enough to prevent for amorphisation.

5. Conclusion

In this study the helium release from zirconolite samples doped with ^{239}Pu, ^{238}Pu and ^{244}Cm has been analyzed. It is shown that the release from amorphised material (^{244}Cm- and ^{238}Pu-doped) is associated with the re-ordering and recrystallisation back into the original structure. It was shown that the helium generated in a crystalline sample pertains up to much higher temperature although it is a much smaller fraction. Natural analogues do not provide enough insights since their thermal histories are not well known usually. The diffusion coefficient in the crystalline zirconolite has been determined from helium implanted specimens and will be assessed from doped material. For matrices doped with short living actinides it can be estimated when the structure will become amorphous and what is the total quantity of helium that will be generated in the sample. By considering the temperature in storage condition it could then be easily estimated if the helium would be retained in the material or released imposing the load in actinides of the host matrix or the design of the next confinement barrier. The next measurement campaign will be devoted to determine precisely the quantity of helium released and answer the question whether all the radiogenic helium was confined in the amorphous structure or not.

Acknowledgements

The authors are thankful to J.Y. Colle and F. Capone for the Knudsen cell measurement and to H. Thiele for the TEM analysis. This work has been achieved within the Joint Research Project 02–32 in the framework of ACTINET, the European network for actinide sciences, supported by the European Commission under Contract No. FI6W-CT-2004-508836.

References

[1] G.J. McCarthy, Nucl. Technol. 32 (1977) 92.
[2] A.E. Ringwood, E.S. Kesson, N.G. Ware, W. Hibberson, A. Major, Nature 278 (1979) 219.
[3] A.E. Ringwood, E.S. Kesson, K.D. Reeve, D.M. Levins, E.J. Ramm, in: R.C.E.a.W. Lutze (Ed.), Radioactive Waste Forms for the Future, Elsevier, North-Holland, Amsterdam, Netherlands, 1988, p. 233.
[4] R.C. Ewing, L. Wang, Nucl. Instrum. Meth. B 65 (1992) 319.
[5] G.R. Lumpkin, R.C. Ewing, Phys. Chem. Miner. 16 (1988) 2.
[6] W.J. Weber, J.W. Wald, H. Matzke, J. Nucl. Mater. 138 (1986) 196.
[7] F.W. Clinard, F.D. Hobbs, C.C. Land, D.L. Peterson, D.L. Rohr, R.B. Roff, J. Nucl. Mater. 105 (1982) 248.
[8] T.A.G. Wiss, J.-P. Hiernaut, P.M.G. Damen, S. Lutique, R. Fromknecht, W.J. Weber, J. Nucl. Mater. 352 (2006) 202.
[9] S.X. Wang, L. Wang, R.C. Ewing, G.S. Was, G.R. Lumpkin, Nucl. Instrum. Meth. B 148 (1999) 704.
[10] K.L. Smith, N.J. Zaluzec, G.R. Lumpkin, J. Nucl. Mater. 250 (1999) 36.
[11] W.J. Weber, J.W. Wald, H. Matzke, Mater. Lett. 3 (1985) 173.
[12] J. Magill, Nuclide.net, an Interactive Environment for Computations on Radionuclides and their Radiation, Springer-Verlag, 2002.
[13] F. Jorion, X. Deschanels, T. Advocat, F. Desmoulière, J.N. Cachia, S. Peuget, D. Roudil, G. Leturcq, Nucl. Sci. Eng. 153 (2006) 1.
[14] C. Ronchi, J.-P. Hiernaut, J. Nucl. Mater. 325 (2003) 1.

[15] T. Wiss, H. Matzke, V.V.R. Rondinella, T. Sonoda, W. Assmann, M. Toulemonde, C. Trautmann, Prog. Nucl. Energ. 38 (2001) 281.
[16] R.C. Ewing, T.J. Headley, J. Nucl. Mater. 119 (1983) 102.
[17] X. Deschanels, V. Picot, B. Glorieux, F. Jorion, S. Peuget, D. Roudil, C. Jegou, V. Broudic, J.N. Cachia, T. Advocat, C. Den Auwer, C. Fillet, J.-P. Coutures, C. Hennig, A. Scheinost, J. Nucl. Mater. 352 (2006) 233.
[18] F.W. Clinard, D.L. Rohr, R.B. Roff, Nucl. Instrum. Meth. B 1 (1984) 581.
[19] F.W. Clinard, D.L. Peterson, D.L. Rohr, F.D. Hobbs, J. Nucl. Mater. 126 (1984) 245.
[20] K.A. Vlasov (Ed.), Geochemistry and Mineralogy of Rare Elements and Genetic Types of their Deposits, Israel Program for Scientific Translation, Jerusalem, 1966, vol. 2.
[21] W. Sinclair, A.E. Ringwood, Geochem. J. 15 (1981) 229.